Active Control of Separation on a Wing With Oscillating Camber

David Munday* and Jamey Jacob†
University of Kentucky
Lexington, Kentucky

Nomenclature

c	Chord length, 20.3 cm
f	Actuation frequency, Hz
f^+	Reduced frequency, $f \cdot c/U$
Re	Reynolds number based on c
U	Freestream velocity
α	Angle of attack, degrees

Introduction

Low Reynolds number effects are significant in the aerodynamics of low speed airfoils, aircraft intended to operate in low-density environments, and small scale lifting surfaces such as insect and bird wings. Current aerodynamic applications include Micro Aerial Vehicles and Unmanned Aerial Vehicles (μAVs and UAVs), as well as aircraft operating at high altitudes or low density atmospheres other than Earth's.

The primary difficulty with the operation of a wing at low Reynolds number is that the flow over the suction surface encounters an adverse pressure gradient at a point at which the boundary layer is quite likely to still be laminar. Since a laminar boundary layer is incapable of negotiating any but the slightest adverse pressure gradient, the flow will inevitably separate. The separated flow then transitions to turbulence, entrains fluid and re-attaches to form a turbulent boundary layer. The resulting structure is the laminar separation bubble, which has been described by Lissaman.[1]

A number of different flow control approaches have been investigated to reduce separation and improve efficiency at low Reynolds numbers.[2] Continuous blowing and sucking have long been shown to have pronounced effects. More recently, intermittent blowing and sucking in the form of synthetic jets have shown their effectiveness, and suggest the presence of optimum values in the range of frequency inputs, which may translate to other oscillatory inputs.[3–5] Mechanical momentum transfer and acoustic excitation have also been explored.

The approach presented herein employs an adaptive wing.[6] Naturally, all practical wings are adaptive in the sense that they use actuators to alter lift coefficient by changing effective profile with a subsequent loss in efficiency. A truly adaptive wing, however, refers to an airfoil which can change its profile to optimally adapt to flow conditions. Similar concepts have been explored in the past, such as the snap-through airfoil which changes local airfoil camber by moving a flexible portion of the pressure surface,[7] or the DARPA smart wing which uses torsional elements to twist the wing.[8] Modern smart materials such as piezoelectric actuators offer great promise in the area of future stall control applications,[9] though simple mechanisms such as buzzing bars have also been shown to be adequate stall control devices.[10] The kind of adaptation which is of primary interest here is one in which the rate of actuation is rapid, and may be able to respond quickly enough to arrest or limit the formation of laminar separation bubbles. At high Re, the unsteady theory of Theodorsen[11] may be utilized to solve such problems (see Duffy *et al.*[12] for an example), but at low Re where viscous forces are predominate, there is no rigorous method to predict the unsteady effects of such rapid actuation and how it will alter separation.

Experiment

The adaptive wing design is based upon a static prototype design constructed by Pinkerton and Moses as a feasibility test for drag reduction.[13] A modular wing was constructed with a base profile of a NACA 4415. Each module has a recess cut in the upper surface, into which a piezoelectric actuator is placed. The actuators are mounted at such an angle that they are even with the un-recessed airfoil section when at their smallest effective radius (when most curved). A thin plastic sheet is then placed over the actuator to smooth the profile, and then the entire assembly is wrapped in a latex membrane to hold it together and provide a seamless outer surface. When the actuator is displaced to its greatest effective radius (closest to being flat) it protrudes through the upper cross-section. The plastic sheet and latex membrane smooth the upper surface increasing the effective camber and moving the point of maximum thickness aft. The device has been more fully described elsewhere.[15]

Experiments with a circular-arc airfoil at low Re suggest that an airfoil with oscillating camber will produce a higher lift coefficient than the same airfoil at any fixed camber setting through separation control.[16] The present experiment attempts to extend this finding to airfoils of more ordinary and more efficient cross-section. The current experiments were conducted with four wing modules, assembled to form a wing with a chord of eight inches and a span of 13 inches giving an aspect ratio of 1.6. This wing was mounted in an 8×16 inch test section in a low-speed low-turbulence wind tunnel. Smoke-wire flow visualization as described in Batill and Mueller is used to mark the outer boundary of separated flow.[17] Displacement of the actuators was measured *in situ* with a Keyance LK-501 laser displacement sensor. These measurements are accurate to within ±5% at all frequencies across the range of interest.

Results

Flow visualization at $Re = 2.5 \cdot 10^4$ and $5.0 \cdot 10^4$ clearly shows large separated flow over the wing with the actuator static ($f^+ = 0$). This is expected at low speeds with a NACA 4415 profile which is not designed for low Reynolds number flight. When the actuator is oscillating, the size of the separated flow is greatly reduced. Figure 1 shows images of the flow visualization for $Re = 2.5 \cdot 10^4$ at two different angles of attack for both uncontrolled and controlled runs where $f^+ = 0$ and $f^+ > 0$, respectively. From the recorded images, the size of the separated region at 70% of chord was measured normal to the surface of the foil by determining the distance from the airfoil surface to the mean location of the first smoke streakline. These measurements are presented in Figures 2 and 3. The instrumental error in these measurements amounts to ± 0.2 mm, or far less than one percent of chord. This is dwarfed by the statistical error, which can best be inferred from examining the scatter in the dynamic data (variation in streakline location). The overall error, then, is within ± 1% of chord.

The static measurements refer to those where the actuator was kept in a stationary state at a number of pre-determined positions. For these an increase in separation as angle of attack increases is seen, which is what would be expected. An increase in separation as Reynolds number decreases is also seen. This is also as one would expect. The main

*Graduate student; Department of Mechanical Engineering; member AIAA. *munday@engr.uky.edu*

†Assistant professor; Department of Mechanical Engineering; senior member AIAA. *jdjacob@uky.edu*

Presented as Paper 2001–0293 at the AIAA 39th Aerospace Sciences Meeting, Reno, NV, Jan. 8–11, 2001. Copyright © 2001 by the American Institute of Aeronautics and Astronautics, Inc. All rights reserved.

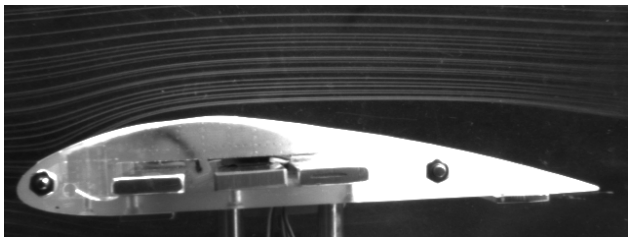

a) $\alpha = 0°$, $f^+ = 0$

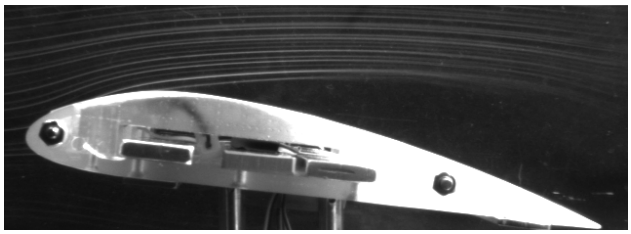

b) $\alpha = 9°$, $f^+ = 0$

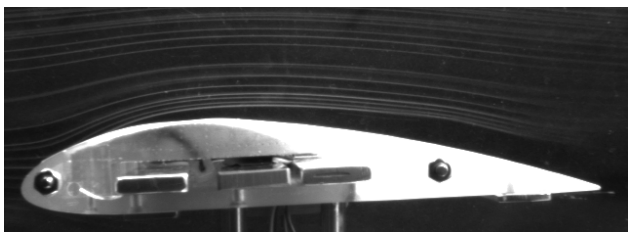

c) $\alpha = 0°$, $f^+ = 1.7$

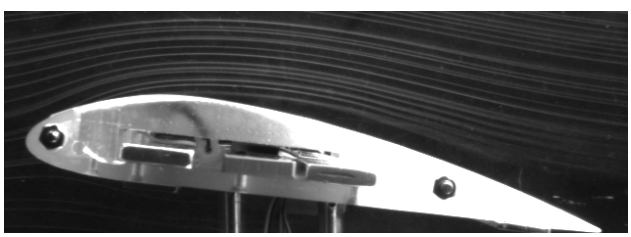

d) $\alpha = 9°$, $f^+ = 5$

Fig. 1 Smoke-wire flow visualization at $Re = 2.5 \cdot 10^4$ for static and actuated cases.

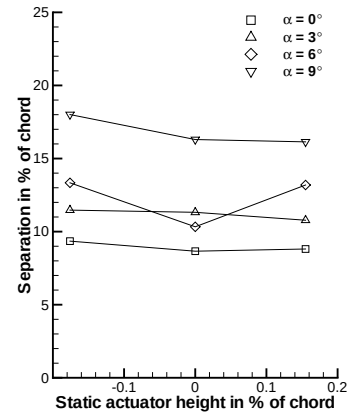

a) $Re = 2.5 \cdot 10^4$.

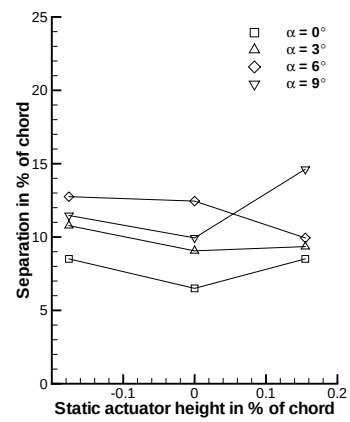

b) $Re = 5.0 \cdot 10^4$.

Fig. 2 Separated flow thickness measured normal to the suction surface at 70% of chord for the static case.

purpose of the static measurements was to provide a direct comparison to the dynamic measurements. To that end the minimum size observed is the value used in Fig. 4, which represents a best case scenario for separated flow over an unactuated airfoil.

Force and PIV measurements of the airfoil with static shape changes were studied at a preliminary stage using solid models over a range of overlapping Re corresponding to the flow visualization observations shown in Fig. 2.[14] Force measurements showed that both coefficients of lift and drag showed a slight increase at intermediate settings of the actuator, with an overall *decrease* in L/D of 6%. Maximum actuator displacement also increased both lift and drag but with an overall *increase* in L/D of 2%. This was confirmed in the PIV measurements where it was revealed that the size of the separation region increased and then decreased with increasing static actuator position. The modest improvement in efficiency did not warrent further investigation of static actuator effects, however. Moment coefficients were not measured.

The dynamic measurements refer to those in which the actuator was oscillated at a given frequency. The amplitude of oscillation was normalized to $\pm$ 0.2 mm measured at $0.3c$. This represents a peak-to-peak displacement of $0.002c$. For frequencies above 70 Hz this normalization could not be maintained without producing destructive sparks along the edges of the actuator or at the attachment points of the electrical leads and measurements at above this frequency were thus taken with reduced maximum displacement. The regions of normalized displacement and non-normalized displacement are noted on Fig. 3. The data is plotted in terms of reduced frequency, f^+, where frequency is normalized by chord length and free-stream velocity, $f^+ = f \cdot c/U$.

Measurements at a chord-based Reynolds number of $2.5 \cdot 10^4$ show that the size of the separated flow is generally reduced with increasing frequency up to the point where normalization is lost. The measurements at $\alpha = 0°$ show a broad minimum around $f^+ = 5$. The measurement at $\alpha = 3°$ may also indicate a minimum before normalization is lost. At higher angles of attack though, where the decrease in separation is more significant, the improvement in performance appears to continue up to the point of loss of normalization. Past this point, where the amplitude of the actuator oscillation diminishes, the performance of the foil degrades at all angles of attack. It cannot be determined from present data whether this increase in separation is due to the decreased amplitude or the increased frequency, but the former is suspected.

Observations at a Reynolds number of $5.0 \cdot 10^4$ show no such degradation in performance past loss of normalization. In the non-normalized range the separation is in the range of $4 - 6\%$ for all frequencies. In the normalized range the same general trend is seen where separation is reduced with increasing frequency. There is a possible shallow minimum at $\alpha = 3°$ and $f^+ = 3$, and another at $\alpha = 6°$ and $f^+ = 3$.

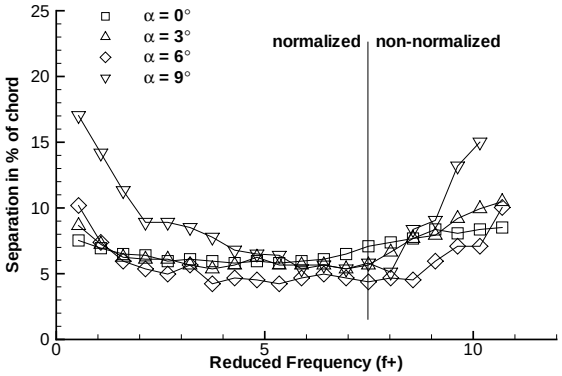

a) $Re = 2.5 \cdot 10^4$.

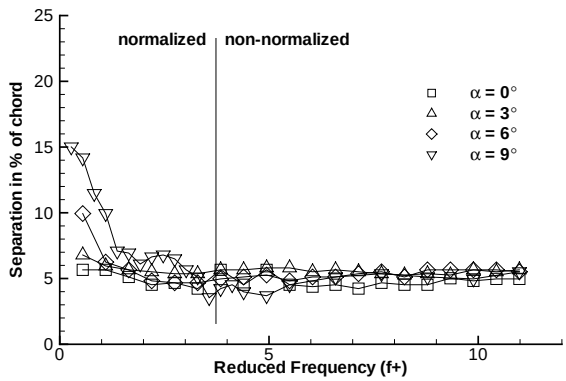

b) $Re = 5.0 \cdot 10^4$.

Fig. 3 Separated flow thickness measured normal to the suction surface at 70% of chord for the dynamic case.

From a more detailed analysis of Fig. 1, it can be shown that the point of separation remains nearly the same when comparing the uncontrolled and controlled cases. Since the region of camber oscillation is downstream of the original separation point, this indicates that the actutation is not affecting the upstream flow but rather is aiding the flow in navigating the adverse pressure graident in the region of separation, most probably by direct energization of the boundary layer. Note that the flow examined here is within the transition range ($Re < 5 \cdot 10^4$).[1] Transition can be located in the flow visualization images and is not observed to significantly change chord-wise location when the flow control is engaged.

Figure 4 shows the minimum observed separation for each combination of α and Re for both the static and dynamic cases. It can be seen from this plot that the application of an oscillatory input holds the size of the separated flow to $4 - 6\%$ of chord. This is, of course, more significant for the cases of higher angle of attack and for lower Reynolds number, where the non-actuated flow has a larger separated region. It remains to be seen if increasing amplitude will further improve performance in this range.

Conclusions

Oscillating the curvature of the upper surface of a NACA 4415 airfoil has been shown through flow visualization to have a pronounced effect in reducing the degree of separation over a foil at the Reynolds numbers of $2.5 \cdot 10^4$ and $5 \cdot 10^4$. Under these conditions the unmodified flow can separate by as much as $0.15c$ or more. Separation, measured at the 70% chord position, was held to $0.04 - 0.06c$ under angles of attack up to 9° by oscillating the upper surface with an amplitude of $0.002c$ and reduced frequencies f^+ ranging

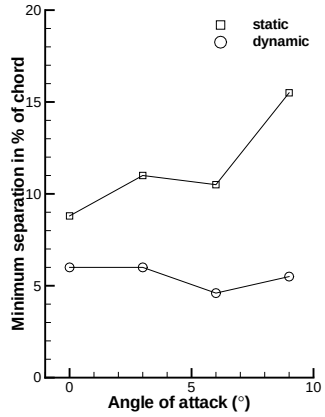

a) $Re = 2.5 \cdot 10^4$.

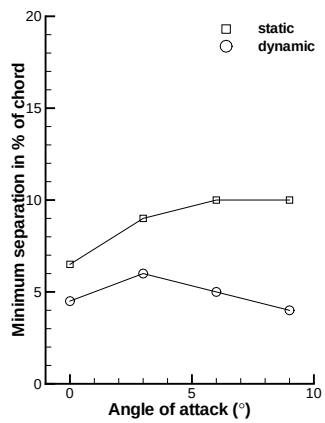

b) $Re = 5.0 \cdot 10^4$.

Fig. 4 Minimum separated flow thickness, static vs. dynamic cases.

from 0 to 11. This represents a reduction in the separated flow size by 30% to 60% as compared to flow over a similarly shaped static wing. This technique shows significant promise and it is expected that further tests will verify an improved efficiency in terms of L/D.

Acknowledgments

This research was supported by the Kentucky Space Grant Consortium.

References

[1] Lissaman, P. B. S., "Low-Reynolds-Number Airfoils," *Annual Review of Fluid Mechanics*, Vol. 15, 1983, pp. 223–39.

[2] Gad-el-Hak, M., *Flow Control: Passive, Active, and Reactive Flow Management.* Cambridge University press, 2000.

[3] Amitay, M., Smith, D. R., Kibens, V., Parekh, D. E., and Glezer, A., "Aerodynamic Flow Control Over an Unconventional Airfoil Using Synthetic Jet Actuators," *AIAA Journal*, Vol. 39, No. 3, 2001, pp. 361–370.

[4] Greenblat, D., and Wygnanski, I., "Dynamic Stall Control by Periodic Excitation, Part 1: NACA 0015 Parametric Study," *Journal of Aircraft*, Vol. 38, No. 3, 2001, pp. 430–438.

[5] Sinha, S. K., "Flow Separation Control with Microflexural Wall Vibrations," *Journal of Aircraft*, Vol. 38, No. 3, 2001, pp. 496–503.

[6] Jacob, J. D., "On the Fluid Dynamics of Adaptive Airfoils," *Proceedings of the 1998 ASME International Mechanical Engineering Congress and Exposition*, Anaheim, CA, 1998.

[7] Duffy, R. E., Dubben, J., Nickerson, J., and Colasante, J., "A Theoretical and Experimental Study of the Snap-Through Airfoil and its Potential as a High Harmonic Control Device," AIAA Paper 88-0668, Jan. 1988.

[8] Kudva, J., Appa, K., Martin, C. A., Jardine, A. P., Sendeckyj, G., Harris, T., McGowan, A., and Lake, R., "Design, Fabrication, and Testing of the DARPA/Wright Lab 'Smart Wing' Wind Tunnel Model," AIAA Paper 97-1198, April 1997.

[9] Seifert, A., Eliahu, S., Greenblatt, D., and Wygnanski, I., "Use of Piezoelectric Actuators for Airfoil Separation Control," *AIAA Journal*, Vol. 36, No. 8, 1998, pp. 1535–1537.

[10] Park, Y. W., Lee, S.-G., Lee, D.-H., and Hong, S., "Stall Control with Local Surface Buzzing on a NACA 0012 Airfoil," *AIAA Journal*, Vol. 39, No. 7, 2001, pp. 1400–1402.

[11] Theodorsen, T., "General Theory of Aerodynamic Stability and the Mechanism of Flutter," NACA TR 496, 1935.

[12] Duffy, R. E., Czajkowski, E. A., and Jaran, C., "Finite Element Approximation to Theororsen's Solution for Non-Steady Aerodynamics of an Airfoil Section," AIAA Paper 84-1640, June 1984.

[13] Pinkerton, T. L. and Moses, R. W., "A Feasibility Study to Control Airfoil Shape Using THUNDER," NASA TM-4767, 1997.

[14] Munday, D., and Jacob, J. D. "Flow Control Experiments for Low-Re Adaptive Airfoils," AIAA Paper 2000-0654, Jan. 2000.

[15] Munday, D., and Jacob, J. D. "Active Control of Separation on a Wing with Conformal Camber," AIAA 2001-0293, Jan. 2001.

[16] Pern, N. J., *Vortex Mitigation Using Adaptive Airfoils.* M. S. Thesis, University of Kentucky, Lexington, Kentucky, 1999.

[17] Batill, S. and Mueller, T. "Visualization of Transition in the Flow Over an Airfoil Using the Smoke Wire Technique," *AIAA Journal*, Vol. 19, No. 3, 1981, pp. 340–345.